Modeling the Dynamics of Cascading Failures in Power Systems

Xi Zhang, Choujun Zhan, and Chi K. Tse, *Fellow, IEEE*

***Abstract*— In this paper, we use a circuit-based power flow model to study the cascading failure propagation process, and combine it with a stochastic model to describe the uncertain failure time instants, producing a model that gives a complete dynamic profile of the cascading failure propagation beginning from a dysfunctioned component and developing eventually to a large-scale blackout. The sequence of failures is determined by voltage and current stresses of individual elements, which are governed by deterministic circuit equations, while the time durations between failures are described by stochastic processes. The use of stochastic processes here addresses the uncertainties in individual components' physical failure mechanisms, which may depend on manufacturing quality and environmental factors. The element failure rate is related to the extent of overloading. A network-based stochastic model is developed to study the failure propagation dynamics of the entire power network. Simulation results show that our model generates dynamic profiles of cascading failures that contain all salient features displayed in historical blackout data. The proposed model thus offers predictive information about occurrences of large-scale blackouts. We further plot cumulative distribution of the blackout size to assess the overall system's robustness. We show that heavier loads increase the likelihood of large blackouts and that small-world network structure would make cascading failure propagate more widely and rapidly than a regular network structure.**

***Index Terms*— Complex network, power system, dynamics of cascading failure, power flow study, stochastic process.**

I. Introduction

ELECTRICITY supply network is an essential part of the infrastructure of modern society. Large power blackouts cause inconvenience to residents in the affected areas as well as considerable economic loss to the community at-large. Power system's security has always been an issue of serious concern among utility providers, infrastructure developers, and policy makers, and is also a topic attracting significant attention of electrical engineers and researchers. The power distribution network is a complex and highly interconnected network, consisting of power apparatus, protection equipment and control systems [1]. Protection equipment is responsible for maintaining reliability through applying switching actions of relays and circuit breakers. Relays are essential auxiliary components in transmission lines, generators, transformers, and other kinds of power apparatus. When a relay detects an abnormal operating condition such as over-current and voltage dip, it will switch off the affected component to remove the fault from the network, thereby preventing further damages and hence ensuring the normal operation of the rest of the system. The on/off states of relays determine the structure of the power network, thus influencing the overall operational state of a power system. Normally the power grid is designed to maintain its power distribution function even when a few elements are removed [2]. However, when the power grid is under stressed conditions, for instance, due to heavy loads and outages of equipment, the removal of some elements may lead to huge disturbances and subsequent tripping of other elements, causing a possible severe blackout [1].

The dynamic cascading failure process in a power grid can be viewed as a sequence of tripping events, leading eventually to power outage affecting a very large area. It has been observed that the 1996 Western North America blackouts [3], the 2003 Northeastern America and Canadian blackouts [4] and other historical blackout data all display a typical profile characterized by a relatively slow initial phase followed by a sharp escalation of cascading failures. Such a universal form of dynamic profiles strongly suggests that a common model can be used to describe the dynamic cascading failure process.

The study of the dynamic propagation of cascading failures provides useful hints for system vulnerability detection, robustness assessment and network control. Recently, Chen *et al.* [5] used a generalized Poisson model, negative binomial model and exponentially accelerated model to generate the probabilities of the propagation of transmission outages which fit the observed historical data. Dobson *et al.* [6], [7] used branching processes to analyze the propagation of cascading failures in power grids. Much of the previous work primarily applied data fitting methods to investigate the statistical characteristics of power systems' blackouts, but fell short of considering the essential electrical circuit operations or the impact of the network structure. Moreover, cascading failures in power grids have also been studied in terms of the sequential trippings of electrical elements in real networks. Among the many switching mechanisms of relays, overloading is the most prominent one and has been widely studied [8]–[13]. In a cascading failure process, the failure of one element leads to power flow redistribution in the grid,

Manuscript received October 12, 2016; revised December 22, 2016; accepted January 19, 2017. Date of publication March 3, 2017; date of current version June 10, 2017. This work was supported by the Hong Kong Research Grants Council GRF under Project PolyU 5258/13E. This paper was recommended by Guest Editor H. Ho-Ching Iu.

X. Zhang and C. K. Tse are with the Department of Electronic and Information Engineering, Hong Kong Polytechnic University, Hong Kong (e-mail: xi.r.zhang@connect.polyu.hk; encktse@polyu.edu.hk).

C. Zhan was with The Hong Kong Polytechnic University, Hong Kong. And now he is with the Department of Electronics Communication and Software Engineering, Nanfang College of Sun Yat-sen University, Guangzhou 510900, China (e-mail: zchoujun2@gmail.com).

Color versions of one or more of the figures in this paper are available online at http://ieeexplore.ieee.org.

Digital Object Identifier 10.1109/JETCAS.2017.2671354

which can cause some other elements to be overloaded. These overloaded electrical elements can then be tripped by their relays, causing another round of failures until the remaining elements are all within their respective operating limits.

Various of tripping sequence settings of the overloaded elements have been explored [9], [10], [14]. Typically, in each round of the cascading simulations, the power flow distribution in the network is computed, and overloaded electrical elements are removed at the same time. The actual time delays and dynamical profiles of the process are not considered in this kind of models, making them unable to simulate the dynamic propagation of a cascading failure. In order to show the dynamic profile, some previous studies made the simple deterministic assumption that the duration for an overloaded element to be tripped is equal to Δt which is given by $\int_t^{t+\Delta t}(f_j(\tau) - \bar{f}_j)d\tau = \Delta o_j$, where f_j is the power flow of overloaded element j, $\bar{f}_j$ is the flow limit and Δo_j is a specific threshold of that element [15], [16].

Considering the complexities and uncertainties in real power grids [17], a few researchers turned to use probabilistic models to characterize the tripping events of the elements in power grids [11], [12], [18]. For instance, Wang *et al.* [11] used a Markov model to study cascading failures, where the trippings of the elements are regarded as *state transitions,* which are memoryless and probabilistic. In Wang *et al.*'s work, the overloaded elements share one same tripping rate, which is much larger than the natural failure rate of the electrical equipment. Alternatively, an overall state transition probability can be determined by considering the maximum capacity of the failed elements and a random tripping process [12]. It is also shown [19] that a component will experience more failures under heavy load conditions. The varying tripping rates for elements under different extents of overloading stress have not been thoroughly considered in the aforementioned stochastic models. Study of essential collective behavior of a power network must be pursued according to the governing physical laws which in the case of power systems should involve circuit-based power flow equations [10] (see Appendix). By suitably combining the power flow study with probabilistic methods for describing inevitable uncertainties, the dynamic profile of cascading failure processes can be realistically revealed, hence offering important predictive information about the occurrence of large-scale blackouts.

In this paper, we study the dynamics of cascading failure propagations in power systems. The key contributions are as follows. First, we apply circuit-based power flow equations to determine the sequence of failures in accordance to the extent of overloadings of individual components. In order to describe the complete dynamic profile, we need to determine the time durations between failures in the propagation sequence. Due to the complexities and uncertainties of the involving physical failure mechanisms of the components (e.g., manufacturing quality, environmental factors, etc.), stochastic processes are used to model the dynamic changes. Then, to study the collective behavior of the entire system in terms of failure propagation in the whole network, an extended chemical master equation (CME) model is used [20], [21]. Based on the CME model, we show that the failure propagation rate of the network is dependent on the sum of individual extents of overloading of all elements in the network. Simulation results show that the cumulative number of failed elements triggered by some initial failures shows a universal growing pattern which is consistent with historical blackout data. Thus, our model can offer insights into the mechanism of cascading propagation in a power system as well as provide predictive information for the failure spreading in the network. Our study also includes the effects of loading conditions and network structure on the extent and rapidity of blackouts in power systems. The UIUC 150 bus system with different consumer load distributions and several types of network structure are studied for comparison purposes. It is shown that heavy load conditions increase the risk of large blackouts in the same power system, and that small-world network structure is more prone to rapid propagation of cascading failures than the regular structure.

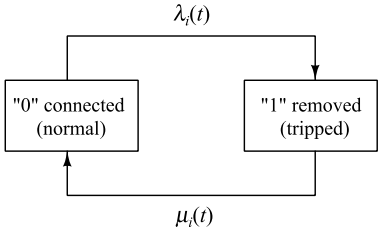

Fig. 1. Dynamic description of failure in terms of state transitions. State "0" is the normal connected state; state "1" is the removed or tripped state.

II. Failure Mechanisms of Components

A power system is composed by various electrical stations connected by transmission lines, and each station or transmission line is protected by protective equipment. In this paper, we model electrical stations as nodes and transmission lines as links, with nodes being connected by links forming a power network [10]. Deterministic power flow equations are used to generate the sequence of failures and their locations. A node or link is a *basic element* of a power network. We refer to an element's tripping event as an *element state transition* (EST). The cascading failure propagation in a power network can be viewed as a sequence of ESTs in the network. In this section, we investigate the state transition behavior of a basic element, and in the next section, we apply probabilistic theory to study the collective transition behavior of the network.

A. Time to Failure of a Basic Element

Let $s_i(t)$ be the state of element i of a given network, and $s_i(t) \in [0, 1]$, with $s_i(t) = 0$ corresponding to a connected element i at time t, and $s_i(t) = 1$ corresponding to a removed (tripped or open-circuited) element i at time t, as shown in Fig. 1. Here, $\lambda_i(t)$ is the rate of transition of node i going from state "0" to "1", and $\mu_i(t)$ is the transition rate from "1" to "0". Then, the future state of an element is solely determined by its present state and the transition rule. Suppose the present time is t, and dt is an infinitesimal time interval. As $s_i(t) \in \{0, 1\}$, $P\{s_i(t + dt) = 1\}$ and $P\{s_i(t + dt) = 0\}$

can be written separately as

$$\begin{aligned} &P[s_i(t+dt)=1] \\ &\quad = P[s_i(t+dt)=1\,|s_i(t)=0\,]P[s_i(t)=0] \\ &\qquad + P[s_i(t+dt)=1\,|s_i(t)=1\,]P[s_i(t)=1] \\ &P[s_i(t+dt)=0] \\ &\quad = P[s_i(t+dt)=0\,|s_i(t)=0\,]P[s_i(t)=0] \\ &\qquad + P[s_i(t+dt)=0\,|s_i(t)=1\,]P[s_i(t)=1] \end{aligned} \tag{1}$$

where $P[s_i(t)=1]$ and $P[s_i(t)=0]$ denote the probability that node i is in state "1" and "0" at time t, respectively; $P[s_i(t+dt)=1\,|s_i(t)=0)\,]$ is the conditional probability that given $s_i(t)=0$ element i transits to state "1" in the time interval $(t, t+dt)$; and $P[s_i(t+dt)=0\,|s_i(t)=1)\,]$ is defined in a likewise manner. Using the state transition rates shown in Fig. 1, $P[s_i(t+dt)=1\,|s_i(t)=0)\,]$ can be written as

$$P[s_i(t+dt)=1\,|s_i(t)=0\,]=\lambda_i(t)dt. \tag{2}$$

Also, $P[s_i(t+dt)=0\,|s_i(t)=0)\,]$ is the probability that given $s_i(t)=0$, element i remains in state "0" in time interval $(t, t+dt)$ (i.e., no state transition occurs). Thus, we have

$$P[s_i(t+dt)=0\,|s_i(t)=0\,]=1-\lambda_i(t)dt. \tag{3}$$

Likewise, we have

$$P[s_i(t+dt)=0\,|s_i(t)=1\,]=\mu_i(t)dt, \tag{4}$$

$$P[s_i(t+dt)=1\,|s_i(t)=0\,]=1-\mu_i(t)dt. \tag{5}$$

B. State Transition Rates of Basic Elements

In this section, we discuss the physical meanings of element state transition rates $\lambda_i(t)$ and $\mu_i(t)$ in a fast cascading failure process. In statistical terms, an event rate refers to the number of events per unit time. Specifically, $\lambda_i(t)$ is the rate of element i becoming disconnected in the network which is caused by either a natural equipment malfunction or tripping by its protective equipment, i.e.,

$$\lambda_i(t)=\lambda_i^0(t)+\lambda_i^1(i) \tag{6}$$

where $\lambda_i^0(t)$ is the equipment malfunctioning rate in the absence of loading stress and its value is constant and derivable from past statistics [16]; and $\lambda_i^1(t)$ is the removal or tripping rate by protective relays and is determined by the (over)-loading condition and the capacity of element i.

Among the many tripping mechanisms of relays [22], [23], power overloading is a dominant one. In this study, we focus on switching actions caused by overloading. When the load of element i is within its capacity, it is assumed to work in the normal condition and will not be removed or tripped by the protective relay, namely $\lambda_i^1(t)=0$. However, when the element exceeds its capacity, there will be a short delay before it is finally removed. The tripping rate is relevant to the extent of overloading. In other words, if there is a large overloading of element i, it will be tripped more rapidly compared to the case of a light overloading [19]. Based on this assumption, we can write $\lambda_i^1(t)$ as

$$\lambda_i^1(t)=\begin{cases} a_i\left(\dfrac{L_i(t)-C_i}{C_i}\right), & \text{if } L_i(t)>C_i \\ 0, & \text{if } L_i(t)\le C_i \end{cases} \tag{7}$$

where $L_i(t)$ is the power loading of element i that can be found from the power flow calculation, C_i is the capacity of that element, and a_i is the basic unit rate (trippings per second). For normal operating condition, $\lambda_i^1=0$. In a cascading failure process, $\lambda_i^1 \gg \lambda_i^0$ [24]. Without loss of generality, we assume that $\lambda_i(t)\approx\lambda_i^1(t)$ in our analysis of cascading failures in power systems.

For the sake of completeness, we also allow a tripped or removed element to be repaired, and hence be restored to its normal connected state. Thus, we define $\mu_i(t)$ as the transition rate of element i going from state "1" to "0" as a result of repair actions or self-healing ability of the power system. In practice, an element's state cannot be switched arbitrarily. Also, the time delay for recovering a tripped element should be considered and can be included in the actual representation of $\mu\ (t)$. This recovery process can be used to study the power restoration process after the power blackout. In this paper, we focus on analyzing the cascading failure process. Thus, considering that not all elements could be repaired in a short time and an element cannot keep changing its status frequently, we take $\mu_i(t)$ as 0 for a fast cascading process.

C. Power Flow Calculation

In addition to equation (7), power flow calculation is still needed for the analysis of cascading failures. Several algorithms and tools are available for computing power flows [25], [26]. The actual power system is a high-order complex nonlinear network, and any abrupt change of network structure can change the power flow distribution, and at the same time cause large transients, oscillations, and bifurcations [27]. Using our definition of state transition of elements, the tripping probability of each element is an integration of the tripping rate (extent of overloading) with time. In this study, we assume that the system can always reach a steady state when tripping occurs and that the transient before the system reaches the next steady state is sufficiently short, making accumulative effects negligible. As far as the propagation of cascading failures is concerned, it suffices to consider blackouts caused by overloading, ignoring the nonlinear characteristics of the circuit elements and possible oscillatory behavior. In our previous work, a model that can accurately track the load change in a power network during a cascading failure has been developed [10]. This model is adopted in our study here. Given information of power consumption, power generation and grid topology, the voltage of each node can be found using

$$A*V=B \tag{8}$$

where A is a matrix describing the power network; $B=\begin{bmatrix}\cdots & I_i & 0 & v_k & 0 & \cdots\end{bmatrix}^T$ with I_i and v_k representing the sink current and voltage of nodes i and k, respectively. A brief description is given in the Appendix and more details can be found in [10]. The current flowing through the transmission line (i, j) can be calculated as

$$I_{ij}=(v_i-v_j)*Y_{ij} \tag{9}$$

where v_i and v_j are voltages of nodes i and j, and Y_{ij} is the admittance of line (i, j). Equation (8) is derived from consideration of circuit laws and thus rigorously describes the behavior of the power network.

III. Failure Propagation in the Network

A power network is represented as an undirected graph G consisting of m elements. The state of G is defined as $S = \{s_1, s_2, ..., s_m\}$, which is a vector containing the states of all m elements. Network G can have 2^m possible network states, and any state transition of an element will lead to a network state transition of G.

The dynamic propagation of cascading failures in G is equivalent to the dynamic evolution of $S(t)$. Given the current state of the network, the network state transition can be described by (i) the time of the next state transition; and (ii) identification of the next element that will transit (be tripped).

A. Basics

First, we consider the network state transitions in an infinitesimal time interval dt. Suppose $S(t) = N_S$, which is a specific network state among the 2^m possible states. Thus, $S(t + dt)$ is the network state after a duration of dt. Only those elements in state "0" may transit, leading to a network state transition. Let Ω_0 be the set of elements in state "0", and Ω_1 be the set of removed (tripped) elements. From elementary probability theory, we have the following basic results:

1) Omitting $O(dt)$, the probability that no element undergoes a state transition after dt can be written as

$$\begin{aligned} &P[S(t+dt) = N_S \,|S(t) = N_S\,] \\ &\quad = \prod_{i\in\Omega_0}[1-\lambda_i(t)dt)] \\ &\quad = 1 - \sum_{i\in\Omega_0}\lambda_i(t)dt + \sum_{x_1,x_2\in\Omega_0}\lambda_{x_1}(t)\lambda_{x_2}(t)(dt)^2 \\ &\qquad - \sum_{x_1,x_2,x_3\in\Omega_0}\lambda_{x_1}(t)\lambda_{x_2}(t)\lambda_{x_3}(t)(dt)^3 + \cdots \\ &\quad = 1 - \sum_{i\in\Omega_0}\lambda_i(t)dt + O(dt) \approx 1 - \sum_{i\in\Omega_0}\lambda_i(t)dt \end{aligned} \quad (10)$$

where $x_1, x_2, \cdots$ are the elements in Ω_0.

2) The probability that only one element state transition (say element k) occurs after dt, i.e., only element k transits, can be written as

$$\begin{aligned} &P[S(t+dt) = M_S \,|S(t) = N_S\,] \\ &\quad = \lambda_k(t)dt \prod_{i\in\Omega_0/\{k\}}[1-\lambda_i(t)dt] \\ &\quad = \lambda_k(t)dt - \sum_{x_1\in\Omega_0/\{k\}}\lambda_k(t)\lambda_{x_1}(t)(dt)^2 \\ &\qquad + \sum_{x_1,x_2\in\Omega_0/\{k\}}\lambda_k(t)\lambda_{x_1}(t)\lambda_{x_2}(t)(dt)^3 + \cdots \\ &\quad = \lambda_k(t)dt + O(dt) \approx \lambda_k(t)dt \end{aligned} \quad (11)$$

where $x_1, x_2, \cdots$ are the elements in $\Omega_0/\{k\}$ and M_S denotes the network state that only one of the "0"-state elements in N_S becomes "1".

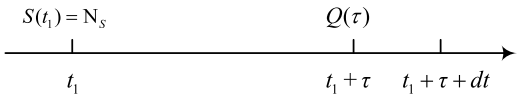

Fig. 2. Time line of network state transitions.

3) The probability that two or more element state transitions occur after dt is given by

$$P[S(t+dt) = R_S \,|S(t) = N_S\,] = 0 \quad (12)$$

where R_S denotes the network state that two or more of the "0"-state elements in N_S become "1". From equation (12), there is at most one element state transition at a time.

B. Extended Gillespie Method

In this section, we derive $S(t)$ using an extended Gillespie method [28], which was used for analyzing coupled chemical reactions [20], [21].

As shown in Fig. 2, the state of the power system at t_1 is N_S, i.e., $S(t_1) = N_S$. Let $Q(\tau)$ denote the probability that given $S(t_1) = N_S$, no transition occurs in $(t_1, t_1 + \tau)$, i.e.,

$$Q(\tau) = P[S(t_1+\tau) = N_S \,|S(t_1) = N_S\,] \quad (13)$$

Similarly, $Q(\tau + dt)$ can be written as

$$\begin{aligned} &Q(\tau+dt) \\ &\quad = P[S(t_1+\tau+dt) = N_S \,|S(t_1) = N_S\,] \\ &\quad = P[S(t_1+\tau+dt) = N_S \,|S(t_1+\tau) = N_S\,]Q(\tau) \end{aligned} \quad (14)$$

Given $S(t_1) = N_S$, power flow calculation can be performed, as described in Section II-C, and $\lambda_i(t_1)$ can be derived based on the settings in Section II-B. If no state transition occurs during time interval $(t_1, t_1 + \tau)$, we have $S(t) = S(t_1)$ and $\lambda_i(t) = \lambda_i(t_1)$ for $t \in (t_1, t_1 + \tau)$. From (10), we get

$$P[S(t_1+\tau+dt) = N_S \,|S(t_1+\tau) = N_S\,] = 1 - \sum_{i\in\Omega_0}\lambda_i(t_1)dt \quad (15)$$

Thus, by putting (15) in (14), we get

$$Q(\tau+dt) = Q(\tau)(1-\lambda^*(t_1)dt) \quad (16)$$

where $\lambda^*(t_1) = \sum_{i\in\Omega_0}\lambda_i(t_1)$. Furthermore, re-arranging (16) and taking the limit $dt \to 0$, we get

$$\begin{aligned} &\frac{dQ(\tau)}{d\tau} = \lim_{dt\to 0}\frac{Q(\tau+dt)-Q(\tau)}{dt} = -\lambda^*(t_1)Q(\tau), \\ &\Rightarrow Q'(\tau) = -\lambda^*(t_1)Q(\tau). \end{aligned} \quad (17)$$

The probability that nothing happens in zero time is one, i.e., $Q(0) = P\{S(t_1) = N_S \,|S(t_1) = N_S\} = 1$. Then, the analytical solution of (17) is

$$Q(\tau) = e^{-\lambda^*(t_1)\tau}. \quad (18)$$

Let $h_i(\tau, dt)$ denote the probability of the event that given $S(t_1) = N_S$, the next transition occurs in the interval $(t_1 + \tau, t_1 + \tau + dt)$ in element i. There are two conditions for this event to occur. The first condition is that there is no state

transition during $(t_1, t_1+\tau)$. The second condition is that a state transition occurs in element i during $(t_1+\tau, t_1+\tau+dt)$. Thus, $h_i(\tau, dt)$ can be written as

$$h_i(\tau, dt) = P[S(t_1+\tau+dt) = M_S \,|S(t_1+\tau) = N_S\,]Q(\tau) \tag{19}$$

Putting (11) and (18) in (19), we get

$$h_i(\tau, dt) = e^{-\lambda^*(t_1)\tau}\lambda_i(t_1)dt \tag{20}$$

Let $H(\tau, dt)$ denote the probability that the next transition occurs in the time interval $(t_1+\tau, t_1+\tau+dt)$, given $S(t_1) = N_S$. It is readily shown that

$$H(\tau, dt) = \sum_{i\in\Omega_0} h_i(\tau, dt) = \lambda^*(t_1)e^{-\lambda^*(t_1)\tau}d\tau \tag{21}$$

Further, let τ denote the time interval between two adjacent network state transitions, and $f(\tau)$ denote the *state transition probability density function* (PDF):

$$f(\tau) = \lim_{dt\to 0}\frac{H(\tau, dt) - H(\tau, 0)}{dt} = \lambda^*(t_1)e^{-\lambda^*(t_1)\tau} \tag{22}$$

i.e.,

$$f(\tau) = \lambda^*(t_1)e^{-\lambda^*(t_1)\tau} \tag{23}$$

The accumulative probability density function that the next transition occurs before time $t_1+\tau$, given $S(t_1) = N_S$, can be written as

$$F(\tau) = \lambda^*(t_1)\int_0^\tau e^{-\lambda^*(t_1)t}dt = 1 - e^{-\lambda^*(t_1)\tau} \tag{24}$$

Note that one can also get $F(\tau)$ from $F(\tau) = 1 - Q(\tau)$.

Equations (23) and (24) show that τ follows an exponential distribution and that the network transition rate is $\lambda^*(t_1)$. Here, $\lambda^*(t_1)$ is the sum of the element state transition rates of all the working elements in the network, and is determined by the sum of the extents of overloading of all the overloaded elements. The time interval τ is expected to be short when $\lambda^*(t_1)$ is large, i.e., the network state transition (cascading process) occurs very rapidly. Thus, the physical meaning of $\lambda^*(t_1)$ can be interpreted as the overloading stress of the entire power system.

In order to include this characteristic in our model, we take the following steps to determine the time of the next network state transition, given $S(t_1) = N_S$:

1) A random number z_1 is generated uniformly in (0,1).
2) Let $F(\tau) = z_1$, and τ is derived as

$$\tau = \frac{ln(1-z_1)}{-\lambda^*(t_1)}. \tag{25}$$

C. Order of State Transition

A number of working elements (elements in Ω_0) can possibly undergo state transition. In our analysis presented in Section III-A, we allow only one element to be removed (tripped) at a time. Pfitzner *et al.* [29] pointed out that the order in which overloaded lines are tripped influences the cascade propagation significantly. In this section, we study the order in which element state transitions take place.

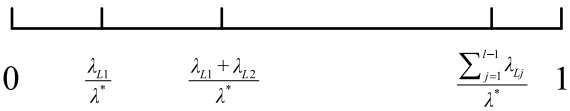

Fig. 3. Relative probability for elements in Ω_0 to be first tripped given $S(t_1) = N_S$.

In our stochastic model, any overloaded element in Ω_0 may be tripped first. From a probabilistic viewpoint, the element with a higher $h_i(\tau, dt)$ will more likely be tripped first. Thus, we define the *relative probability* for element i ($i \in \Omega_0$) to be tripped first as:

$$rf_i = \frac{h_i(\tau, dt)}{H(\tau, dt)} = \frac{\lambda_i(t_1)}{\lambda^*(t_1)}. \tag{26}$$

where $\lambda^*(t_1) = \sum_{i\in\Omega_0}\lambda_i(t_1)$. Our model can incorporate this tripping order using the following steps:

1) A random number z_2 is generated uniformly in (0,1).
2) Suppose there are l overloaded elements in Ω_0. With no loss of generality and for ease of referral, let these overloaded elements be elements $L1, L2, \ldots, Lj, \ldots, Ll$. Fig. 3 shows the relative probability of an overloaded element in Ω_0 to be first tripped, given that $S(t_1) = N_S$.
3) The jth element in Ω_0 is selected to be tripped according to

$$\sum_{k=0}^{j-1}\frac{\lambda_{Lk}}{\lambda^*} \leqslant z_2 < \sum_{k=0}^{j}\frac{\lambda_{Lk}}{\lambda^*} \tag{27}$$

where $\lambda_{L0} = 0$.

IV. Cascading Failure Simulations and Parameters

In this section we describe the simulation algorithm and some important characterizing parameters of our model that are relevant to predicting the occurrence of power blackouts.

A. Simulation Algorithm

Fig. 4 shows the flow chart for simulating the cascading failure process which can be summarized as follows:

1) *Initial Settings:* At the start of the simulation, all voltages at the power generation stations, currents flowing into the consumer nodes, admittances of the transmission lines, and capacities of elements are set.
2) *Initial Failure:* An initial failure is planted by removing one element from the network, which triggers the cascading failure process.
3) *Iterative Process:* Based on $S(t)$, we remove the tripped elements from the network, and keep all elements whose states is "0". The remaining network may be disconnected, forming so-called islands, due to the removal of the tripped elements. For a disconnected sub-network (island) containing no generator node, all elements within it would have no access to power and all power flows become zero. All nodes in this sub-network are *unserved*. Note that these elements are not tripped, and their states are still "0". Moreover, for a sub-network containing at least one generator node, equation (8) can

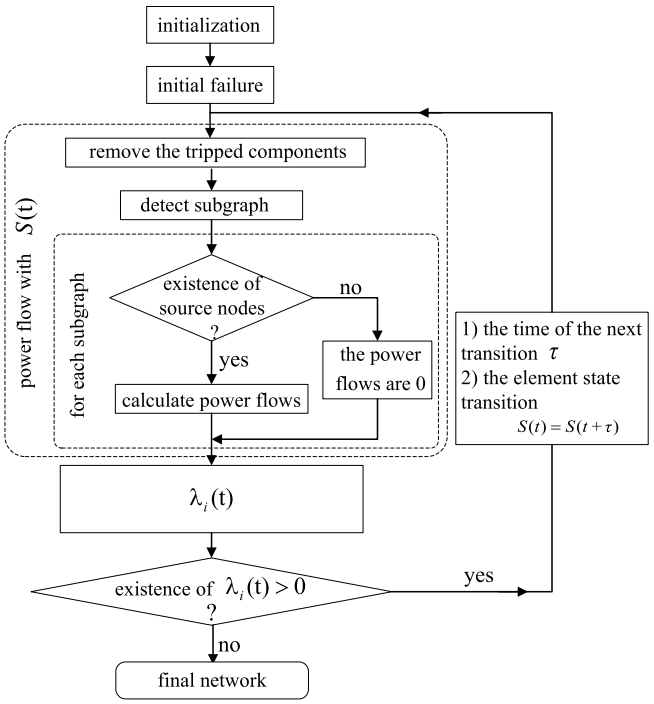

Fig. 4. Flow chart for simulating cascading failure.

be used to compute the power flow distribution in this sub-network. Power flows of all the "0"-state elements in G can be computed, and the tripping rate of each element λ_i can be obtained using (7). If all tripping rates are positive, we determine the next network state. Specifically, we first determine the time of the next network state transition using (25), and determine the element in Ω_0 that will be tripped next. The network state transition is determined using (27). Then, we update $S(t) = S(t + \tau)$, and iterate the process until all the transition rates are found to be zero (i.e., no overloaded elements). With no more overloaded elements in the network, no state transition will occur and $S(t)$ is a stable state. We can then end the simulation and get the final network.

B. Parameter Settings and Metrics

The time of the initial failure is set as zero, and the time of the final network state transition (after which there are no overloaded elements in the network, and the network state enters a stable point) is t_{final}. Using the above algorithm, we can simulate the dynamic profile of $S(t)$ for power network G, from $t = 0$ to $t = t_{\text{final}}$. For $t > t_{\text{final}}$, $S(t)$ remains unchanged. The dynamic profile of $S(t)$ is thus the dynamic propagation of cascading failures in the network. In order to better represent and visualize the characteristics of the dynamics of a cascading failure, we use the following metrics, which are extracted from $S(t)$.

We propose several metrics to investigate the cascading failure in a power system.

First, to characterize the propagation profile of a cascading failure in a power system, the cumulative number of tripped

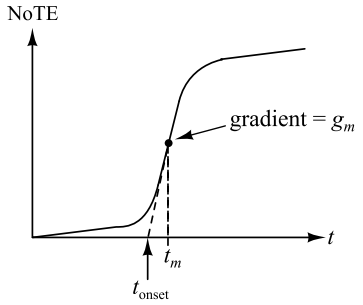

Fig. 5. Typical propagation profile and onset time t_{onset}. Maximum propagation rate g_m occurs at $t = t_m$.

elements at time t (NoTE(t)) is used. Here, we take NoTE(t) as the number of "1"-state elements in $S(t)$. Also, the number of elements not served is another important metric used to measure the blackout size. As the power grid's operation depends on the connection of the elements, the tripping of some elements in the network can disconnect the grid and island the consumer nodes from the power sources. These nodes are being deprived of power, and are labelled as *unserved nodes* in our analysis. We use NoUN(t) to denote the number of cumulative unserved nodes at t. To find NoUN(t), we remove the tripped elements in G, and identify all sub-networks in the remaining part of G. The consumer nodes that are isolated from generators are all unserved nodes.

Furthermore, during a cascading failure process, it is particularly important to track the growing rate of the number of failed or tripped elements, i.e., the frequency of removal or tripping of overloaded elements. Specifically, any rapid increase in the frequency of removal of overloaded elements is a precursor to an onset of a large blackout. Thus, a metric that effectively gives the critical time from which tripping begins to take place more rapidly is extremely relevant to prevention of power blackouts. This metric, called *onset time* (t_{onset}) here, can simply be defined as the time after which the propagation rate of the cascading failure increases rapidly, as depicted in Fig. 5. In other words, t_{onset} is a critical time point before which remedial control and protection actions should be applied to the power grid. After t_{onset}, the power grid undergoes a short phase of very rapid tripping of overloaded elements leading to large power blackout within a very short time. To compute the onset time, we identify the maximum rate of the growing profile by solving $d^2\text{NoTE}(t)/dt^2 = 0$, which gives $t = t_{\text{m}}$ as the time point where the growing rate is highest. Assuming that the value of $d\text{NoTE}(t)/dt$ at $t = t_m$ is g_m and the initial phase has a very slow growing rate, the onset time is simply given by

$$t_{\text{onset}} = t_m - \frac{\text{NoTE}(t_m)}{g_m} \tag{28}$$

In practice, we can use any handy algorithm to find t_{onset}, for instance, by locating the time instant where $d\text{NoTE}(t)/dt$ starts to increase rapidly. Section V-B offers one simple algorithm.

Finally, to characterize the general severity in the event of a possible blackout, we use the following statistical metric. Suppose a large number of cascading failure cases, initialized

by failures of different elements in the network, are simulated. The probability that the blackout size of a randomly picked case is larger than a chosen threshold BS (Blackout Size) is given by

$$P[x(t) \geq \text{BS}] = \frac{n[x(t) \geq \text{BS}]}{n} \tag{29}$$

where $x(t)$ can be NoTE(t) or NoUN(t), n is number of the total blackout cases simulated, and $n[x(t) \geq \text{BS}]$ is the number of cases whose blackout size at t is larger than BS. Based on (29), we can evaluate the cumulative blackout size distribution of a network to reveal the probability (risk) of having a blackout of a specific level of severity in a given network.

V. Application Case Study

In this section, we simulate cascading failures in the UIUC 150 Bus System using the model proposed above. The UIUC 150 Bus is a power test case offered by Illinois Center for a Smarter Electric Grid at UIUC [30]. It contains 150 buses and 217 links that operate in 3 different voltage base values. We merge the parallel lines that connect the same two buses into one link, resulting in 203 links in our simulation. We assume that the current sinks of the consumer buses given in the UIUC 150 Bus are the normal load demands of these consumers. The voltages of generators are all 1.04 p.u. based on the data in the test case.

From the historical blackout reports [3], [4], one can find that the tripped elements are mostly generators, transmission lines and transformers. Thus, in our simulation, we set current limits for the transmission lines, transformers and the generators according to $C_i = (1+\alpha) * I_i(\text{normal})$, where $I_i(\text{normal})$ is the current flowing through a transformer or a transmission line, or the total current flowing out of a generator under normal load demand condition; α is the safety margin and is set to 0.2. The current limits of other elements (consumer buses and distribution buses) are set to values that are large enough to avoid tripping during a cascading failure.

A. Dynamics of Cascading Failure Propagation

We first study the failure spreading during a blackout process. Fig. 6(a) shows the profile of cumulative tripped elements of the blackout in the Western North American system in July 1996 [3]. The blackout started from the failure of the 345 kV Jim Bridger-Kinport line (the time of that initial failure is 0 in the figure). As shown in the Fig. 6(a), NoTE grew very slowly, at the initial phase, until the failing of the 230 kV Brownlee-Boise Bench line at 1600 seconds after the initial failure. Then, the cascading failure speeded up abruptly, and within 380 seconds, NoTE reached 33 from 6 at the end of the initial phase. Finally, the cascading failure settled at a final state where 34 major elements were tripped, depriving 10% consumers of the Western interconnection area from access to electrical power. Fig. 6(b) shows the profile of NoTE in another blackout of the same power system that occurred in August 1996. The cascading failure was triggered by the failure of the 500 kV Big Eddy-Ostrander line, and then continued with a sequence of tripping of elements. In almost

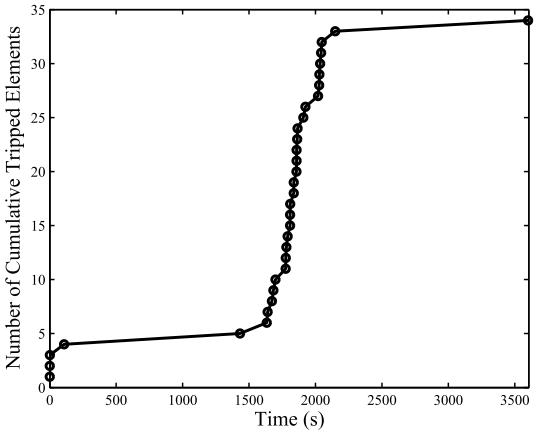

(a)

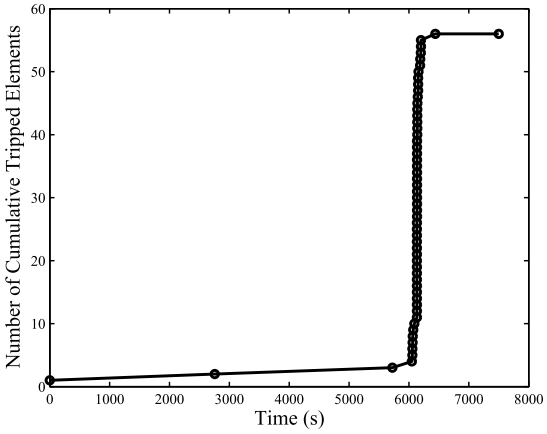

(b)

Fig. 6. Propagation profile of the Western North America power blackout in (a) July 1996; (b) August 1996.

the same fashion, the cascading failure propagated slowly at the beginning, but 6000 seconds later, the propagation rate accelerated sharply. The main propagation finished in 120 seconds. The 2003 American-Canada blackout [4] also showed a similar growing pattern, with NoTE growing very slowly for the initial 4 hours and then accelerating rapidly to its final state. The rapid increase in NoTE occurred in a few minutes, which was a small fraction of the whole cascading period (0, t_{final}).

In the following, we use the proposed stochastic model to simulate the dynamic propagation of cascading failures triggered by the failure of one single line. First, we simulate 100 different propagation profiles of the cascading failure process triggered by the initial failure of line (2, 21), under a normal load demand condition and the condition with 5% increase in load demands. Note that when the loading of the power system is increased by 5% and $S(t = 0) = \mathbf{0}$, there are no overloaded elements, i.e., the 5% increase in load demands will not cause any outage in the power grid. From the data of historical blackouts, the time duration of the failure propagation is usually between 1 hour and 4 hours. In this simulation, we use a uniform a_i for all the elements in the UIUC 150 Bus system, and fit a_i to make the

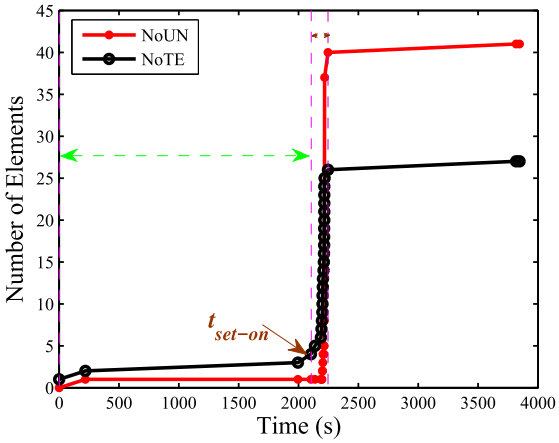

(a)

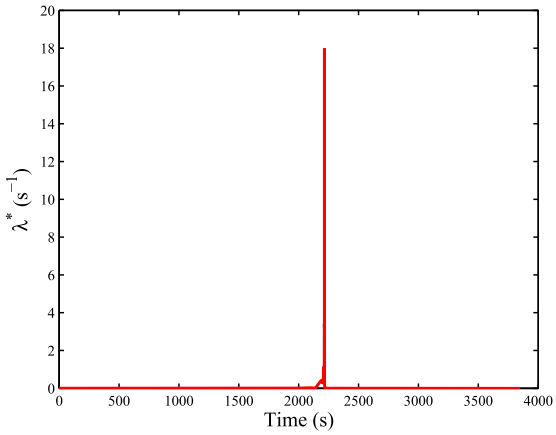

(b)

Fig. 7. Simulation of the dynamics of a cascading failure event in the UIUC 150 Power System caused by an initial failure of line (2, 21). (a) NoTE and NoUN; (b) λ^*.

TABLE I
SIMULATION RESULTS FOR THE CASCADING FAILURE TRIGGERED BY THE FAILURE OF LINE (2, 21)

Loading condition	NoTE(t_{final})	NoUN(t_{final})	t_{final} (s)
Normal loading	5	2	967
5% Load increase	25	36	3600

averaged t_{final} of the 100 simulated results under the condition of 5% increase in load demands to be 3600 s. Thus, a_i is set as 0.035 s^{-1} in our simulation. Table I lists the averaged simulated values of NoTE(t_{final}), NoUN(t_{final}) and t_{final}. From Table I, we see that under a normal load demand condition, the failure of line (2, 21) will not cause severe disturbance to the power system. When the network is stressed by heavier loads, the failure of the same transmission line can lead to a large blackout in the power system.

Table II lists the sequence of the element tripping events in one simulated cascading failure process under the condition of 5% increase in load demand. We plot the profiles of NoTE and NoUN in Fig. 7(a), which display the same typical

TABLE II
SEQUENCE OF ELEMENT TRIPPING EVENTS

Sequence Number	Time	Unit/Line
1	0.000s	Line (2, 21) is tripped.
2	220.035s	Line (2, 14) is tripped.
3	1995.531s	Line (108, 101) is tripped.
4	2104.394s	Line (96, 102) is tripped.
5	2137.931s	Line (8, 23) is tripped.
6	2187.153s	Line (142, 101) is tripped.
7	2191.648s	Line (3, 19) is tripped.
8	2195.871s	Line (10, 25) is tripped.
9	2199.473s	Line (144, 116) is tripped.
10	2199.971s	Line (15, 17) is tripped.
11	2200.115s	Line (9, 39) is tripped.
12	2203.461s	Line (144,117) is tripped.
13	2204.694s	Generator 1 is tripped.
14	2209.551s	Line (88, 147) is tripped.
15	2211.713s	Line (16, 26) is tripped.
16	2212.815s	Generator 118 is tripped.
17	2213.497s	Line (89, 26) is tripped.
18	2217.194s	Line (114, 119) is tripped.
19	2214.603s	Line (68, 85) is tripped.
20	2214.909s	Line (137, 95) is tripped.
21	2215.02s	Line (148, 95) is tripped.
22	2215.073s	Line (65, 73) is tripped.
23	2215.649s	Line (22, 29) is tripped.
24	2215.669s	Line (6, 28) is tripped.
25	2217.261	Line (17, 21) is tripped.
26	2246.489s	Line (69, 87) is tripped.
27	3817.977s	Line (69, 70) is tripped.

growing pattern as the historical blackout data. Using equation (23), the growth rate of the cascading failure is determined by $\lambda^*(t)$. Fig. 7(b) shows the values of $\lambda^*(t)$ throughout the simulated cascading process. Initially, the value of $\lambda^*(t)$ is relatively small, until the breakdown of some critical elements, its value increases very rapidly. This means that the power network operates under a high overloading stress. When the stress comes down again, the propagation slows down. The tripping of elements ceases when $\lambda^*(t)$ reduces to 0, and the network reaches its final condition. The consistency of our simulated cascading failure process with the historical data verifies the validity of our model in describing realistic blackout processes. The following two key issues should be noted.

(1) We use stochastic methods to investigate the cascading failure propagation. Our model takes into consideration the high complexities as well as uncertainties of the involving mechanisms which can be investigated with probabilistic methods. The tripping rates of the elements are related to the overloading extents of the corresponding elements and the more heavily overloaded ones will be more likely to be tripped first. Equations (25) and (27) incorporate these considerations. Thus, for the same system and same initial failure, different simulations may yield different results due to the stochastic nature of the model. Fig. 7 is one particular simulation run of the UIUC 150 Bus with initial failure of line (2, 21). Furthermore, Figs. 8 (a)-(f) show results derived from 6 other

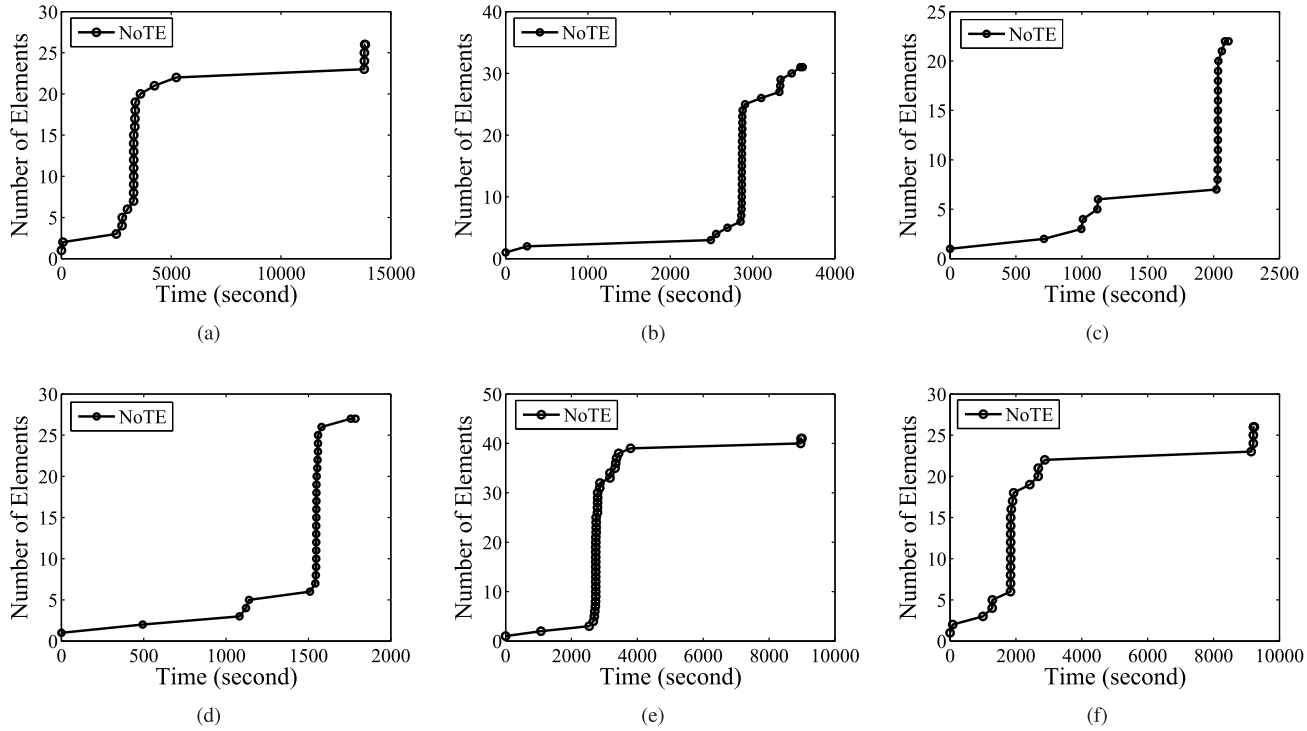

Fig. 8. Simulation of failure propagations in UIUC 150 Bus power system with initial tripping of line $(2, 21)$ using the proposed model. (a)-(f) Six separate simulation runs.

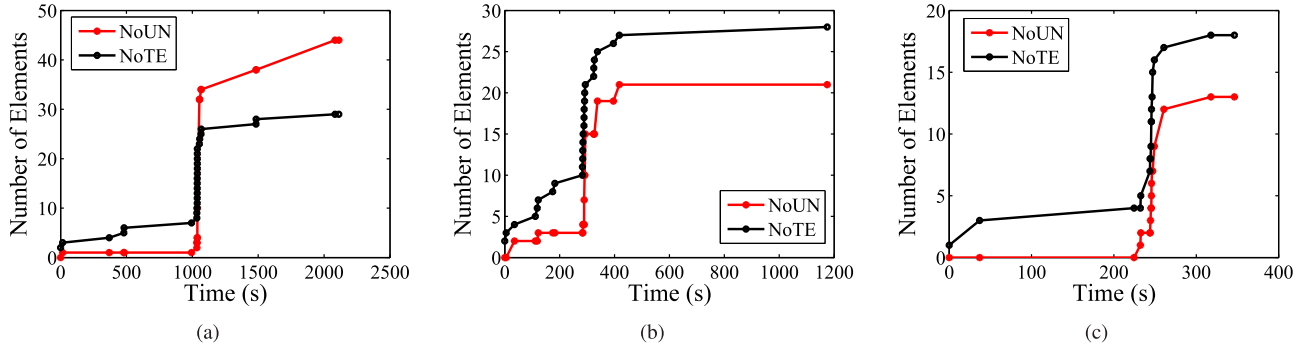

Fig. 9. Simulation of failure propagation initiated by (a) failure of line (2, 14) in UIUC 150 Bus; (b) failure of line (34, 35) in UIUC 150 Bus; (c) failure of line (103, 105) in IEEE 118 Bus.

simulation runs. From Fig. 8, we can see that these 6 sets of results share the same characteristic profile, where the growing rate of the blackout size is uneven and a relatively slow initial phase is followed by a sharp escalation of cascading failures.

(2) From our simulations, we observe cascading failure patterns as shown in Fig. 7. Figs. 9 (a) and (b) show the simulated cascading failure propagation in the UIUC 150 Bus initiated by the failure of line (2, 14) and the failure of line (34, 35), respectively. Fig. 9 (c) shows the simulated cascading failure propagation in the IEEE 118 Bus initiated by the failure of line (103, 105). It should be noted that not all initial failures will generate such cascading failure profiles. In fact, the initial failure of some elements will not cause further cascading failures at all. Another extreme case is that initial failure of some crucially important element in the network will make all other elements to be unserved instantly. For instance, the initial failure arises from a generator which is the only generating unit in its power network. Moreover, the failure propagation profile shown in Fig. 7 is unique for power systems, which is determined by the specific failure spreading mechanism. Such profile is not normally observed in other failure spreading mechanisms, such as disease propagations in human networks, rumour spreading on the Internet, and so on.

B. Blackout Onset Time

To evaluate t_{onset}, we adopt an intuitive algorithm that locates the time point at which NoTE begins to escalate rapidly. Suppose this time point is t_k which corresponds to the time when the kth element is tripped. The gradient of NoTE before this time point is $g_i = (k-1)/t_k$, and the gradient of NoTE after this time point is $g_m = w/(t_{k+w} - t_k)$, where w is an arbitrary additional number of elements tripped after the kth time point for the purpose of computing the gradient.

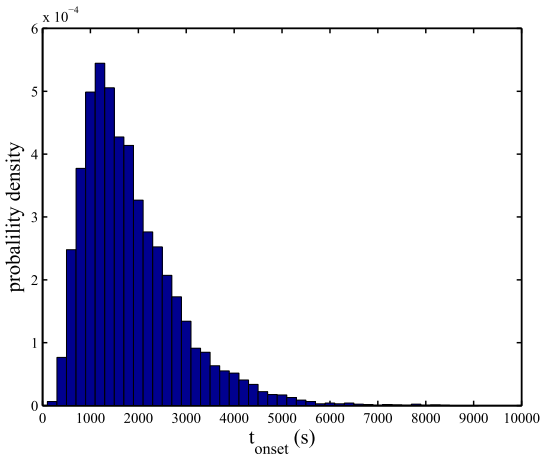

Fig. 10. Probability density function of t_{onset}.

TABLE III
CONFIDENCE INTERVALS OF t_{onset}

Confidence Level	Confidence Interval (sec)
90%	(543, 3747)
95%	(451, 4327)
99%	(286, 5705)

We compare the two gradients, and if $g_m > \gamma\, g_i$, where $\gamma > 0$, we accept this kth time point as the onset time.

We perform 10,000 simulations of cascading failures triggered by removal of line (2, 21). In our algorithm, we use $\omega = 10$ and $\gamma = 50$ to find t_{onset} of these 10,000 simulation runs and analyze the probability density function of t_{onset}. From Fig. 10, we see that there is a peak in the interval (1200 s,1400 s), implying that t_{onset} is more likely to be around 1300 s. Also, Monte Carlo method is applied to derive the confidence interval of t_{onset} for three different confidence levels, as listed in Table III. It should be noted that the t_{onset} distribution shown in Fig. 10 is only valid for the cascading failures in the UIUC 150 Bus power system with initial failure of line (2, 21). Different systems should have different t_{onset} distributions, which should be derived from computation on the specific power systems.

C. Effects of Heavy Load Demands

Another common characteristic of the three historical blackouts is that they all took place in the hot summer when the power demand is high. In this section, we investigate the overall influence of load demands on blackout risk of a power network. The cumulative blackout size distribution is used to indicate the risk of severe power blackouts of the power system.

Under a normal load demand condition, we simulate 10 profiles of cascading failure triggered by the failure of each line. Thus, we have altogether 2030 blackout cases for the UIUC 150 Bus System. Then, we analyze the profile data of these 2030 blackouts. The cumulative distributions of NoTE(t_{final}) and NoUN(t_{final}) are plotted using equation (29). These simulations are repeated for the conditions that the load demands are increased by various percentages. Figs. 11(a) and (b) show the cumulative distributions for NoTE(t_{final}) and NoUN(t_{final}) of the UIUC 150 Bus System under several different load demand conditions. Specifically, all simulated cascading failures will result in NoTE(t) > 0, as any cascading failure simulation has a tripped element as initial failure. Thus, for BS threshold = 0, $P[x(t) \geq 0] = 1$ where x(t) is NoTE(t). We see that under a normal load condition, the probability of large blackouts of the UIUC 150 Bus System is relatively low. However, when the load demands are increased, the probability of large blackouts increase significantly. We also observe that the probability of having severe blackouts does not grow in linearly with the growth of load demands. From Figs. 11(a) and (b), $P[x(t_{\text{final}}) \geq \text{BS}]$ grows relatively slowly relatively when the load demand increases by less than 5%, but more rapidly when the load demand increases by 5% to 10%.

D. Effects of Network Structure

It has been shown that the network topology plays a significant role in determining the dynamics of propagation and spreading of disease or information in networks [31]. For example, infectious disease spreads more readily in small-world networks than in regular ones [31]. It is shown that the topological characteristics of many real-world power systems are not uniform [32]. Thus, it is meaningful to investigate the relationship between network structure and functional properties of power systems, and to identify better connectivity styles. However, since the mechanism of infectious disease or information spreading is totally different from that of failure cascading in power systems, the conclusion derived in prior studies cannot be applied directly to the power systems directly.

Regular networks and small-world networks are used as test power systems for comparison purposes. A regular network is generated with 150 nodes, each node's degree being 4. We allocate 30 generators in the regular network, whose voltages are set as 1.04 p.u. The remaining nodes are consumer nodes, each sinking 0.3 p.u. of current, and the admittances of all links in this network are set as 2×10^3 p.u. Then, we generate 3 small-world networks by rewiring the links in the regular network with rewiring probabilities 0.1, 0.2 and 0.3 [31].

For each test network, we increase the consumers' load demands by 5%, and then simulate 10 profiles of the cascading failure initiated by the failure (removal) of each line. We plot the cumulative blackout size distributions for the 4 networks based on equation (29). Fig. 12(d) shows the cumulative distribution of NoTN(t_{final}), and we see that the risk of large final blackouts is higher for small-world networks than for regular ones. In order to show the speed of the propagations in these networks, we plot the accumulative distributions of NoTE at different time points. Figs. 12(a), (b) and (c) show the cumulative distributions of NoTE at 100 s, 500 s and 1000 s, respectively. For the same duration $[0, t_0]$, a higher value of $P\{\text{NoTE}(t_0) \geq \text{BS}\}$ for the same BS indicates a faster speed of cascading. From Fig. 12, we can conclusion that the

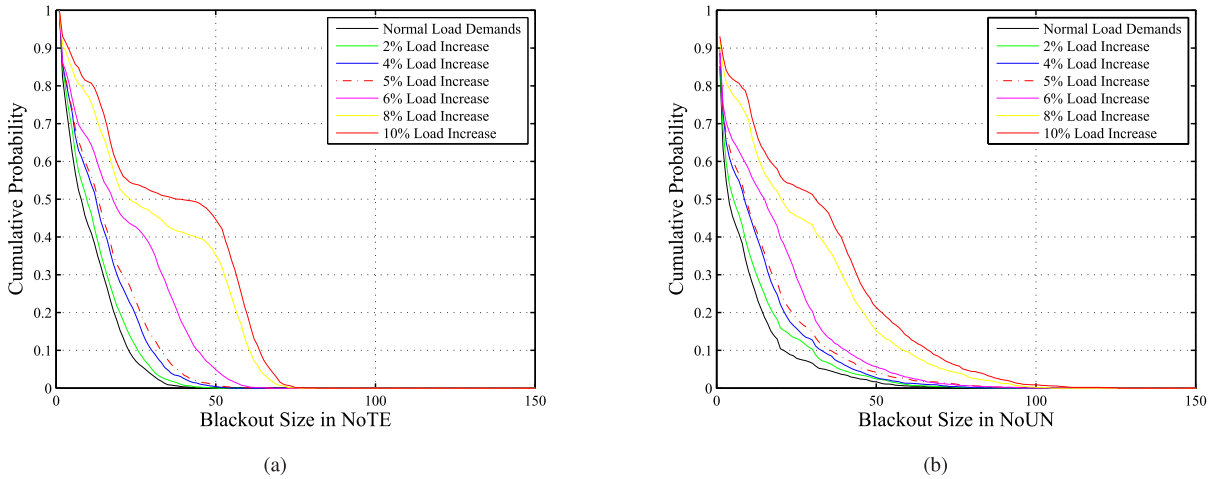

Fig. 11. Cumulative blackout size distributions of UIUC 150 Power System. Blackout size measured in (a) NoTE; (b) NoUN.

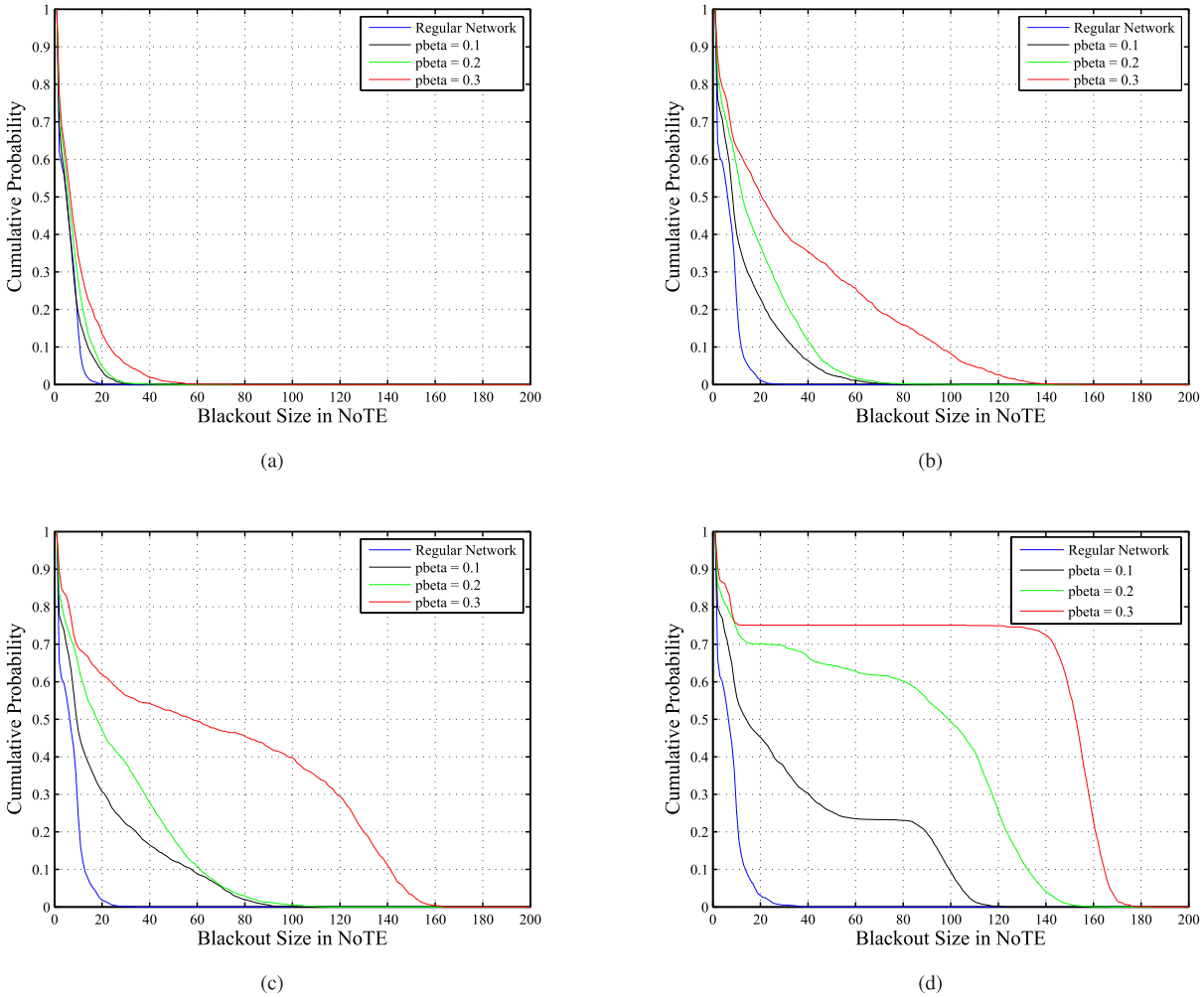

Fig. 12. Cumulative blackout size distributions. (a) $t = 100$ s; (b) $t = 500$ s; (c) $t = 1000$ s; (d) $t = t_{\text{final}}$. "pbeta" is rewiring probability for generating small-world networks.

cascading failure propagates faster in small-world networks than in regular networks.

VI. Conclusions

In this paper, we develop a model to investigate the dynamics of the cascading failure processes in power systems, combining deterministic power flow equations and stochastic time duration descriptions. An extended chemical master equation method is adopted to analyze the network failure dynamics. It has been verified that the model produces propagation profiles that contain the key features displayed in historical blackout data. We studied the UIUC 150 Bus system and

a few important representative network structures with the model, and identified the effects of heavy load demands and network structure on the rapidity of propagation of possible blackouts. We also develop metrics to evaluate the risk of large-scale blackouts in terms of cumulative blackout size distributions. The model described in this paper thus provides predictive information for possible power blackout events in power systems.

APPENDIX
POWER FLOW CALCULATION

Four kinds of nodes are considered in a power network: consumer nodes, distribution nodes, transformer nodes and generation nodes. Voltage and currents in the network are computed according to the kinds of nodes as described below.

A. Consumer Nodes (Loads)

A consumer node i dissipates power, and at the circuit level, it sinks current I_i and is unregulated. The current value is negative as the node consumes power, i.e.,

$$\begin{bmatrix} -Y_{i1} & \cdots & Y_{ii} & \cdots & -Y_{in} \end{bmatrix} * V = I_i \tag{30}$$

where $V = \begin{bmatrix} \cdots & v_i & v_j & v_k & v_h & \cdots \end{bmatrix}^T$; v_n and I_n are the voltage and external injected current at node n, respectively; Y_{ij} is the admittance of the transmission line connecting nodes i and j; and $Y_{ii} = \sum_{j \neq i} Y_{ij}$. If there is no transmission line between nodes i and j, $Y_{ij} = 0$.

B. Distribution Nodes

A distribution node j is modelled as a transfer node without any external injected current.

$$\begin{bmatrix} -Y_{j1} & \cdots & Y_{jj} & \cdots & -Y_{jn} \end{bmatrix} * V = 0 \tag{31}$$

C. Generation Nodes

A generation node k is a fixed voltage source. The current emerging from this node depends on its voltage, the power consumption of other nodes and the network topology. The nodal equation is

$$\begin{bmatrix} 0 & \cdots & y_k & \cdots & 0 \end{bmatrix} * V = v_k \tag{32}$$

where $y_k = 1$, and v_k is the voltage of node k.

D. Transformer Nodes

Transformer nodes connect the high-voltage grids with mid-voltage or low-voltage grids. Usually two equations are required to describe the relations of electrical parameters around a transformer node h. In this study, we perform our analysis in per unit (p.u.). Thus, one equation is sufficient:

$$\begin{bmatrix} -Y_{h1} & \cdots & Y_{hh} & \cdots & -Y_{hn} \end{bmatrix} * V = 0 \tag{33}$$

Combining equations (30) to (33), we get the following power system equation:

$$A * V = B \tag{34}$$

where A is the collection of all the row vectors in the equations of all nodes, and $B = \begin{bmatrix} \cdots & I_i & 0 & v_k & 0 & \cdots \end{bmatrix}^T$.

REFERENCES

[1] S. H. Horowitz and A. G. Phadke, *Power System Relaying*. New York, NY, USA: Wiley, 2008.

[2] M. Rausand and A. Høyland, *System Reliability Theory: Models, Statistical Methods, and Applications*, 2nd ed. New York, NY, USA: Wiley, 2004.

[3] E. C. Eakeley *et al.*, "1996 system disturbances," North Amer. Elect. Rel. Council, Disturb. Anal. Working Group, Atlanta, GA, USA, Tech. Rep., 2002. [Online]. Available: http://www.nerc.com/pa/rrm/ea/System%20Disturbance%20Reports%20DL/1996SystemDisturbance.pdf

[4] U.S.-Canada Power System Outage Task Force, "Final report on the August 14, 2003 blackout in the United States and Canada: Causes and recommendations," U.S. Dept. Energy Nat. Res. Canada, Tech. Rep., 2004. [Online]. Available: https://www3.epa.gov/region1/npdes/merrimackstation/pdfs/ar/AR-1165.pdf

[5] Q. Chen, C. Jiang, W. Qiu, and J. D. McCalley, "Probability models for estimating the probabilities of cascading outages in high-voltage transmission network," *IEEE Trans. Power Syst.*, vol. 21, no. 3, pp. 1423–1431, Aug. 2006.

[6] I. Dobson, B. A. Carreras, and D. E. Newman, "Branching process models for the exponentially increasing portions of cascading failure blackouts," in *Proc. 39th Annu. IEEE Hawaii Int. Conf. Syst. Sci.*, Jan. 2005, p. 64.

[7] I. Dobson, "Estimating the propagation and extent of cascading line outages from utility data with a branching process," *IEEE Trans. Power Syst.*, vol. 27, no. 4, pp. 2146–2155, Feb. 2012.

[8] I. Dobson, B. A. Carreras, V. E. Lynch, and D. E. Newman, "An initial model for complex dynamics in electric power system blackouts," in *Proc. 34th Annu. IEEE Hawaii Int. Conf. Syst. Sci.*, Jan. 2001, pp. 710–718.

[9] S. Pahwa, C. Scoglio, and A. Scala, "Abruptness of cascade failures in power grids," *Sci. Rep.*, vol. 4, Jan. 2014, Art. no. 3694.

[10] X. Zhang and C. K. Tse, "Assessment of robustness of power systems from a network perspective," *IEEE Trans. Emerg. Sel. Topics Circuits Syst.*, vol. 5, no. 3, pp. 456–464, Sep. 2015.

[11] Z. Wang, A. Scaglione, and R. J. Thomas, "A Markov-transition model for cascading failures in power grids," in *Proc. 45th IEEE Hawaii Int. Conf. Syst. Sci.*, Jan. 2012, pp. 2115–2124.

[12] M. Rahnamay-Naeini, Z. Wang, N. Ghani, A. Mammoli, and M. M. Hayat, "Stochastic analysis of cascading-failure dynamics in power grids," *IEEE Trans. Power Syst.*, vol. 29, no. 4, pp. 1767–1779, Jul. 2014.

[13] O. Yağan, "Robustness of power systems under a democratic-fiber-bundle-like model," *Phys. Rev. E, Stat. Phys. Plasmas Fluids Relat. Interdiscip. Top.*, vol. 91, no. 6, p. 062811, 2015.

[14] P. Crucitti, V. Latora, and M. Marchiori, "A topological analysis of the Italian electric power grid," *Phys. A, Statist. Mech. Appl.*, vol. 338, nos. 1–2, pp. 92–97, 2004.

[15] M. J. Eppstein and P. D. H. Hines, "A 'random chemistry' algorithm for identifying collections of multiple contingencies that initiate cascading failure," *IEEE Trans. Power Syst.*, vol. 27, no. 3, pp. 1698–1705, Aug. 2012.

[16] P. Rezaei, P. D. H. Hines, and M. J. Eppstein, "Estimating cascading failure risk with random chemistry," *IEEE Trans. Power Syst.*, vol. 30, no. 5, pp. 2726–2735, Sep. 2015.

[17] H. M. Merrill and A. J. Wood, "Risk and uncertainty in power system planning," *Int. J. Elect. Power Energy Syst.*, vol. 13, no. 2, pp. 81–90, Feb. 1991.

[18] R. Yao *et al.* (Mar. 2016). "Risk assessment of multi-timescale cascading outages based on Markovian tree search." [Online]. Available: https://arxiv.org/abs/1603.03935

[19] Y. Sun, P. Wang, L. Cheng, and H. Liu, "Operational reliability assessment of power systems considering condition-dependent failure rate," *IET Generat., Transmiss. Distrib.*, vol. 4, no. 1, pp. 60–72, Jan. 2010.

[20] D. T. Gillespie, "A general method for numerically simulating the stochastic time evolution of coupled chemical reactions," *J. Comput. Phys.*, vol. 22, no. 4, pp. 403–434, Dec. 1976.

[21] D. T. Gillespie, "Exact stochastic simulation of coupled chemical reactions," *J. Phys. Chem.*, vol. 81, no. 25, pp. 2340–2361, 1977.

[22] K. Bae and J. S. Thorp, "A stochastic study of hidden failures in power system protection," *Decision Support Syst.*, vol. 24, nos. 3–4, pp. 259–268, Jan. 1999.

[23] F. Yang, A. P. S. Meliopoulos, G. J. Cokkinides, and Q. B. Dam, "Effects of protection system hidden failures on bulk power system reliability," in *Proc. 38th IEEE North Amer. Power Symp.*, 2006, pp. 517–523.

[24] J. Chen, J. S. Thorp, and M. Parashar, "Analysis of electric power system disturbance data," in *Proc. 34th Annu. IEEE Hawaii Int. Conf. Syst. Sci.*, Jan. 2001, pp. 738–744.
[25] A. R. Bergen and V. Vittal, *Power Systems Analysis*. Upper Saddle River, NJ, USA: Prentice-Hall, 1999.
[26] R. D. Zimmerman, C. E. Murillo-Sánchez, and R. J. Thomas, "MATPOWER: Steady-state operations, planning, and analysis tools for power systems research and education," *IEEE Trans. Power Syst.*, vol. 26, no. 1, pp. 12–19, Feb. 2011.
[27] F. Milano, L. Vanfretti, and J. C. Morataya, "An open source power system virtual laboratory: The PSAT case and experience," *IEEE Trans. Educ.*, vol. 51, no. 1, pp. 17–23, Feb. 2008.
[28] C. Zhan, C. K. Tse, and M. Small, "A general stochastic model for studying time evolution of transition networks," *Phys. A, Statist. Mech. Appl.*, vol. 464, pp. 198–210, Dec. 2016.
[29] R. Pfitzner, K. Turitsyn, and M. Chertkov. (Apr. 2011). "Controlled tripping of overheated lines mitigates power outages." [Online]. Available: https://arxiv.org/abs/1104.4558
[30] *UIUC 150-Bus System*, accessed on Jul. 2016. [Online]. Available: http://icseg.iti.illinois.edu/synthetic-power-cases/uiuc-150-bus-system/
[31] D. J. Watts and S. H. Strogatz, "Collective dynamics of 'small-world' networks," *Nature*, vol. 393, no. 6684, pp. 440–442, 1998.
[32] G. A. Pagani and M. Aiello, "The power grid as a complex network: A survey," *Phys. A, Statist. Mech. Appl.*, vol. 392, no. 11, pp. 2688–2700, 2013.

Xi Zhang received the B.Eng. degree in electrical engineering from Beijing Jiaotong University, Beijing, China, in 2013. He is currently pursuing the Ph.D. degree with the Department of Electronic and Information Engineering, The Hong Kong Polytechnic University, Hong Kong.

His research interests include nonlinear analysis of power systems, modeling of electrical networks, and applications of complex networks in the assessment of robustness of power systems.

Choujun Zhan received the B.S. degree in automatic control engineering from Sun Yat-sen University, Guangzhou, China, in 2007, and the Ph.D. degree in electronic engineering from City University of Hong Kong in 2012. He was a Post-Doctoral Fellow with The Hong Kong Polytechnic University. Since 2016, he has been an Associate Professor with the Department of Electronic Communication and Software Engineering, Nanfang College of Sun Yat-Sen University, Guangzhou, China. His research interests include complex networks, collective human behavior and systems biology.

Chi K. Tse (M'90–SM'97–F'06) received the B.Eng. (Hons.) degree in electrical engineering and the Ph.D. degree from the University of Melbourne, Australia, in 1987 and 1991, respectively.

He served as Head of the Department of Electronic and Information Engineering, The Hong Kong Polytechnic University, Hong Kong, from 2005 to 2012, where he is currently Chair Professor. He has authored/co-authored ten books, 20 book chapters, and over 500 papers in research journals and conference proceedings, and holds five U.S. patents. He received a number of research and industry awards, including the Prize Paper Awards by the IEEE TRANSACTIONS ON POWER ELECTRONICS in 2001 and 2015, the Best paper Award by the *International Journal of Circuit Theory and Applications* in 2003, the *RISP Journal of Signal Processing* Best Paper Award in 2014, two Gold Medals at the International Inventions Exhibition in Geneva in 2009 and 2013, a Silver Medal at the International Invention Innovation Competition in Canada in 2016, and a number of recognitions by the academic and research communities, including honorary professorship by several Chinese and Australian universities, the Chang Jiang Scholar Chair Professorship, the IEEE Distinguished Lectureship, the Distinguished Research Fellowship by the University of Calgary, the Gledden Fellowship and International Distinguished Professorship-at-Large by the University of Western Australia. He received the President's Award for Outstanding Research Performance twice, the Faculty Research Grant Achievement Award twice, the Faculty Best Researcher Award, and several teaching awards with The Hong Kong Polytechnic University.

Dr. Tse serves as panel member of the Hong Kong Research Grants Council and NSFC, and member of several professional and government committees. He is on the Editorial Boards of a few other journals. He has served and serves as the Editor-in-Chief of the IEEE TRANSACTIONS ON CIRCUITS AND SYSTEMS II (2016–2017), the *IEEE Circuits and Systems Magazine* (2012–2015), the Editor-in-Chief of the IEEE CIRCUITS AND SYSTEMS SOCIETY NEWSLETTER (since 2007), an Associate Editor of three IEEE Journal/Transactions, and the Editor of the *International Journal of Circuit Theory and Applications*.